ON THE DETERMINATION OF EXTERNAL FORCES -- APPLICATION TO THE CALIBRATION OF AN ELECTROMAGNETIC ACTUATOR

Izhak Bucher and Moshe Rozenstein
mebucher@tx.technion.ac.it
Faculty of Mechanical Engineering, Technion, Haifa 32000, ISRAEL

ABSTRACT

A method for obtaining an accurate estimate of forces acting upon a vibrating structure is derived in this paper. The method was developed as a means for calibrating an electromagnetic excitation device where the electromagnetic force was sought to be estimated. The unique features of the proposed method are: (a) Compensation of inertial effects; (b) Based on indirect measurement of forces and displacements in conjunction with an accurate dynamical model. The precise account of inertia and elastic effects allows us to model the relationship between the actuall applied forces and various parameters affecting the external forces. In the case of an electromagnetic device those will be ai -gap, current and magnetic flux. The lack of information in this case had lead us to a threefold approach where experimental data is combined with an analytical approach togethe with state-of-the-art measurement-equipment techniques. The necessity to obtain an accurate account of the distribution of inertia in the structure necessitates a precise spatial model extracted by means of a scanning lase - Doppler sensor. The analytical part involves the estimation of Lagrange multipliers with the extended principal of virtual work.

INTRODUCTION

The problem of estimating the magnitude of dynamically applied external forces has man applications and is considered difficult to solve. The main difficulty stems from the fact that forces are distributed and cannot be measured directly. Current state-of-the art measurement equipment allows us to measure forces at discrete locations while response can be measured to a very fine scale (e.g. with the aid of laser scanning sensors). The problem of estimating dynamic forces from measured response is considered ill posed.

The present work attempts to overcome the inherent difficulty in estimating external forces while taking into the account the dynamics of the intermediate structure and its internal distributed forces. The developed expressions provide some insight into the problem of actuator calibration and the anticipated errors due to distributed elastic and inertia properties.

The interest in solving this problem has risen as an electro-magnetic force device needed to be calibrated. In the calibration process, the current, air-gap and magnetic flux were measured. At this stage the proposed procedure was used to estimate the forces exerted by the electromagnetic exciter upon a vibrating structure.

MOTIVATION AND GENERAL DESCRIPTION OF THE PROBLEM

Non-contacting magnetic excitation is on e of the natural means to apply forces on a rotating media. In the current application, an actuator applying forces on a rotating flexible disc was designed. In this case, the gap between the magnetic poles and the vibrating medium may change considerabl and therefore a linearised model may lead to incorrect results. A horseshoe type actuator was used and the drawing of this device is depicted in figure 1.

In dynamic testing of vibration structures, whether rotating or non-rotating, it is important to control the spectral contents of the applied force. When rotating machines are considered, this requirement is even more important as a rotating machine may exhibit many supe - and sub-harmonics of an applied pure-sine force. The harmonics can be the result of non-linea behaviour of the supports or due to the fact that the rotating device in not perfectly axi - symmetric leading to periodic variation of the mass and stiffness properties (BUCHER EWINS, 1997). The ability to apply a pure sinusoidal force is thus important when one wishes to obtain a precise model. Such an actuator can be used for diagnostic purposes (see BUCHER AND SEIBOLD, 1998) and once more spectral

purity is important in this case. The ability to apply a pure sinusoidal force relies the abilit to obtain a precise dynamic model as a function of the operating conditions, e.g. measurable electrical quantities (current, flux) and mechanical quantities, e.g. displacement or air-gap.

Electrodynamic equations

Simplified analysis of t he magnetic force, leads to an expression for the applied force:

$$f = K\frac{i^2}{s^2} \qquad (1)$$

Where K is a constant, i current in the coils, s air gap.

K is a function of the area of the poles A, the number of turns N, the permeabilit - μ,μ_0

The magnetic force can also be expressed as a function of the magnetic flux,

$$f = K_\phi \phi_e^2 \qquad (2)$$

Where K_ϕ is a constant depending upon A and the permeabilit $-\mu,\mu_0$

In reality, le akage and eddy currents would result in a more complicated expression fo the magnetic force thus a 'black-box' approach was taken to construct an in-situ model of the actuator. For that purpose, the current, ai -gap and magnetic flux were measured in t he experimental system that is illustrated below:

In reality, leakage and eddy currents would result in a more complicated expression fo the magnetic force thus a 'black-box' approach was taken to construct an in-situ model of the actuator. For that purpose, the current, ai -gap and magnetic flux were measured in the experimental system that is illustrated below:

Equations of motion of the elastic structure

The equations of motion are developed for the specific example that is shown here, bu t are more general in scope. In this example the elastic structure is modelled as a beam simpl supported at the force gauges.

Due to inertia forces of the elastic structure, the reaction forces ($_1$ R$_2$ in figure 3) do not depend only on the magnetic for ces (F_1 F_2 in figure 3). An expression relating the magnetic forces to the measured quantities (F_1 F_2 s_1 s_2 in figure 3) is developed below.

FOR THE COMPLETE SYSTEM

relate the measured reaction forces to the measured quantities. In this method, fictitious degrees of freedom are added at the force gauges and after the principal of virtual work is invoked these artificial degrees of freedom are forced to zero. Figure 4 shows the added fictitious DOFs - a_1, a_2 (degrees of freedom) as well as the elastic displacement of the beam. We assume that $w(x,t)$ can be expressed as a superposition of modes:

$$w(x,t) = \sum_n \phi_n(x) q_n(t) \qquad (3)$$

thus the displacement includi ng the fictitious DOFs, becomes

$$\tilde{w}(x,t) = \frac{a_2(t)}{L}x + a_1(t)\frac{L-x}{L} + \sum_n \phi_n(x) q_n(t) \qquad (4)$$

that, $\sum_r \left(\frac{d}{dt}\frac{\partial L}{\partial \dot{q}_r} - \frac{\partial L}{\partial q_r} \right) \delta q_r = \delta W$, where $L = T - V$ and T is the kinetic energy while V represents the potential energy. W - represents the external work performed by non - conservative forces (BARUH, 1999).

The sought reactions are found in this approach by obtaining the equations that are related to the fictitious displacements and forcing them to zero. Mathematically we write:

$$\left\{ \frac{\partial}{\partial \delta a_r} \left[\sum_r \left(\frac{d}{dt}\frac{\partial L}{\partial \dot{a}_r} - \frac{\partial L}{\partial a_r} \right) \delta a_r - \delta W \right] \right\}_{a_i = 0} = 0$$

$$i = 1,2,.. \qquad (5)$$

Using equation 4, we may write according to BARUH, 1999).

$$T = \frac{1}{2}\int_0^L \rho A \left(\frac{\partial \tilde{w}(x,t)}{\partial t} \right)^2 dx$$

$$V = \frac{1}{2}\int_0^L EI \left(\frac{\partial^2 \tilde{w}(x,t)}{\partial x^2} \right)^2 dx \qquad (6)$$

The virtual work performed on the elastic beam equals:

$$\delta W(x,t) = R_2 \delta a_2(t) + R_1 \delta a_1(t) + \sum_m F_m(t)\, \delta \tilde{w}(x_m,t) \qquad (7)$$

Substituting equations 4,6 in equation 5 and isolating the equations of a_i $i = 1,2$:

$$R_i = \frac{\partial}{\partial \delta a_i(t)} \left(\frac{d}{dt}\frac{\partial}{\partial \dot{a}_i(t)} \frac{1}{2}\int_0^L \rho A \left(\frac{\partial \tilde{w}(x,t)}{\partial t} \right)^2 dx \delta a_i(t) \right) - \sum_m F_m(t)\, \delta \tilde{w}(x_m,t) \qquad (8)$$

also, substituting equation 4 in equation 7 :

$$R_1 = \sum_n \ddot{q}_n(t)\int_0^L \rho A\left(\frac{L-x}{L}\right)\phi_n(x)dx - \\ -F_1(t)\frac{L-L_2}{L} - F_2(t)\frac{L-L_3}{L} \quad (9)$$

Similarly for R2, we have

$$R_2(t) = \int_0^L \rho A\sum_n \phi_n(x)\ddot{q}_n(t)\left(\frac{x}{L}\right)dx - \\ -F_1(t)\frac{L_2}{L} - F_2(t)\frac{L_3}{L} \quad (10)$$

Finally the magnetic forces can be expressed as :

$$\begin{pmatrix} F_1(t) \\ F_2(t) \end{pmatrix} = \left(\begin{pmatrix} \sum_n \ddot{q}_n(t)\int_0^L \rho A\left(\frac{L-x}{L}\right)\phi_n(x)dx \\ \sum_n \ddot{q}_n(t)\int_0^L \rho A\left(\frac{x}{L}\right)\phi_n(x)dx \end{pmatrix} - \begin{pmatrix} R_1(t) \\ R_2(t) \end{pmatrix} \right)$$

$$\left[\tilde{L}\right] = L\begin{bmatrix} L-L_2 & L-L_3 \\ L_2 & L_3 \end{bmatrix}^{-1} \quad (11)$$

Summary

Equation 10 shows that the magnetic forces are directly related to the force gauges measurements, R_1 R_2 but also depend on a weighted expression of inertia forces.

The estimation of the inertia forces and thei comparison with directly computed magnetic forces (according to equations 1 and 2) is developed below.

Estimating the inertia distribu ion

A scanning laser interferometer was used to estimate $\phi_n(x)$ in equation 3. Due to the nonlinear behaviour of the coupled electromagnet-elastic beam system, a Fourie series was fitted to each of the temporal measurements and for a sinusoidal current the

$$w(x,t) = \sum_n \phi_n(x)\left(A_n \cos n\omega t + B_n \sin n\omega t\right) \quad (12)$$

At every point along the beam, this model was fitted as shown in figure 5.

Figure 6 allowed us to simplify equation 12 into

$$w(x,t) = \phi(x)\sum_n \left(A_n \cos n\omega t + B_n \sin n\omega t\right) \quad (13)$$

3.1.1 Reconstructing the generalized co-ordinates $q_n(t)$ in equation 3

As there are several displacement sensors $s_i(t)$ (that are postioned along the beam (see figure 1 and 3) we have redandunt information and the equalit

$$s_i(t) = w(x_i,t) = \phi(x_i)q_1(t) \text{ ,i=1,2} \quad (14)$$

leads to a least squares approximation of $q_1(t)$:

$$q_1(t) = \frac{\phi(L_1)s_1(t) + \phi(L_4)s_2(t)}{\phi(L_1)^2 + \phi(L_4)^2} \quad (15)$$

where L_1, L_4 are the locations of the gap sensors.

With the parametric model of the temporal response (equation 13) and the measured $\phi(x)$ (see figure 6), the two inertia terms in equation 11 can be computed and the magnetic forces can be reconstructed. The reconstructed generalized co-ordinate is depicted in figure 7.

COMPARISON OF THE MECHANICALLY RECONSTRUCTED MAGNETIC FORCE TO THEIR ELECTRICALLY COMPUTED COUNTERPARTS

Given an estimate of the magnetic force that is based upon mechanical parameters it is possible to compare the results to the electrically obtained ones in equations 1 and 2. Direct computation of equations1 and 2 with the measured current and flux respectivel showed significant deviation that varied as a function of frequency, DC current, amplitude of vibration and the alternating part of the current.

It was found that equation 1 should be replaced by (a still rather simplified expression)

$$F(t-\tau) = \alpha\frac{I^2}{s^2}(t) + \beta \quad (16)$$

Where α, β, τ are the gain, offset and time (phase) lag (respectively).

The ability to independently estimate the magnetic force, allowed us to curve -fit the parameters of equation 16. As an illustration figure 8 presents the estimated phase delay.

Examining figure 6 we can notice that the phase (time) lag depend on several parameters, most notably on the AC amplitude of the current. The simple model in equation 1 does not explain this fact. Running these tests, it was empirically found that the gain α can be expressed as a function of frequency and the DC part of the current:

$$\alpha = \begin{bmatrix} i_{DC} & 1 \end{bmatrix}\begin{bmatrix} a_1^{11} & a_0^{11} \\ a_1^{10} & a_0^{10} \end{bmatrix}\begin{bmatrix} f \\ 1 \end{bmatrix} \quad (17)$$

For an accurate estimation of the magnetic force, equation 11 was found necessary as α was changed by as much as 50% in the range of up to 200Hz.

With this generalized linear model, good fit was obtained as illustrated in figu e 9.

CONCLUSION AND FUTURE WORK

A method to obtain a precise estimate of magnetic forces based upon indirect measurements was presented. A parametric model of the temporal and the spatial response with an accurate measurement of the mechanical response was used to estimate the affect of inertia on a calibration device. A brief demonstration of the proposed method to empirically calibrate and tune the various parameters of an electrical model was presented. The aim of this work is to generate precise model of the magnetic force to allo real-time compensation of coupling effects appearing in highly flexible rotating discs. The method is more general in scope than what was presented here and can be used to approach the difficult problem of indirect force estimation.

REFERENCES

1. BARUH H., 1999, *Analaytical Dynamics*, McGraw-Hill internationa enditions, Singapor
2. BUCHER I. AND EWINS D.J., 1997, "Multi-dimensional Decomposition of Time-Varying Vibration response Signals in rotating machinery", Mechanical Systems and Signal Processing, Vol. 12 No. 4, 576 -601, July
3. BUCHER I. AND SEIBOLD S. A two-stage approach for enhanced diagnosis of rotating machines
Rotor Dynamics, Darmstadt, Germany, September, pp. 338-349.
4. CALKIN M. G., 1996, *Lagrangian and Hamiltonian mechanics*, World scientific publishing Co Pte Ldt
5. GERADIN M. AND RIXEN D., 1994, Mechanical Vibration, *Wiley,NY*
6. UDWADIA F. W. AND KALABA R. E., 1996, *Analytical dynamics*, Cambridge universit press

FIGURES

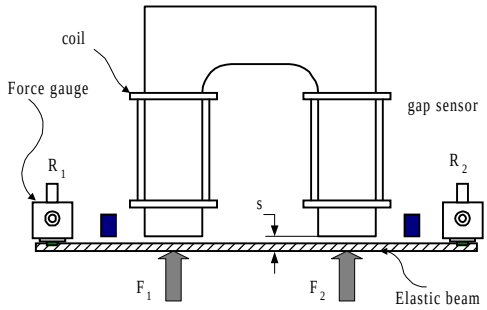

Figure 1. Elect o-magnetic actuator detail

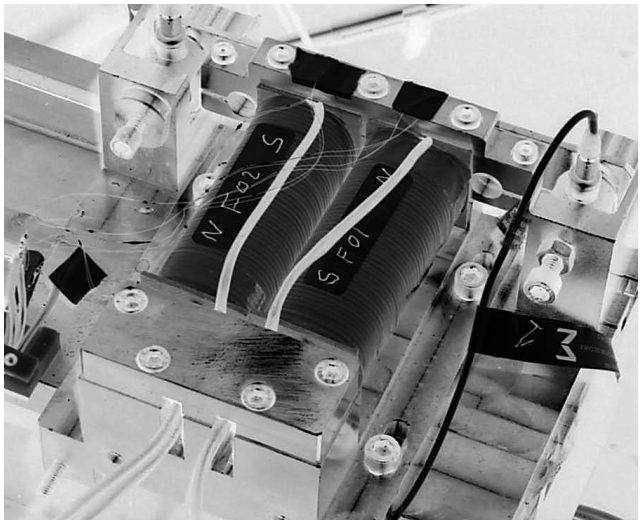

Figure 2 Photograph of the experimental system

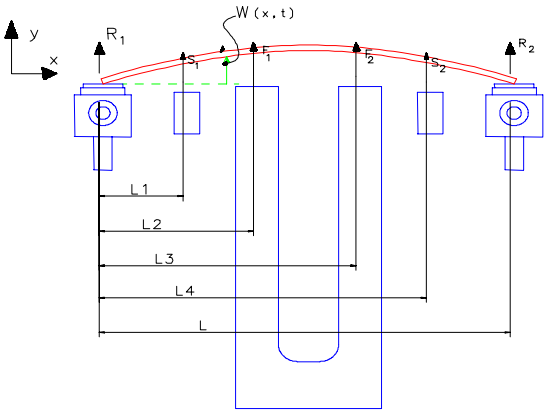

Figure 3 Coordinates of Force gauges, sensors (s_1 s_2 at L_1, L_4), magnetic forces (F_1 F_2 at L_2, L_3), and the Ractions at force gauges - R_1 R_2

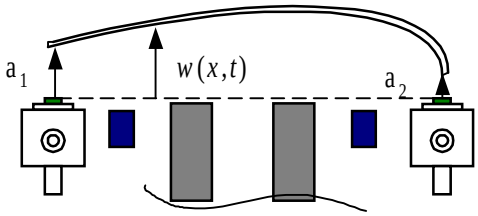

Figure 4 Elastic deflection $w(x,t)$ and fictitious DOFs, a_1, a_2

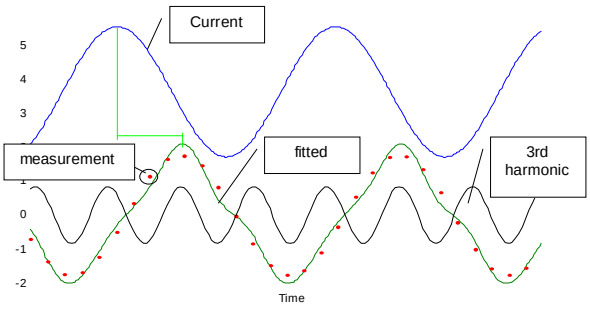

Figure 5. Time histories of the measured current and displacements Vs. the fitted Fourier series.

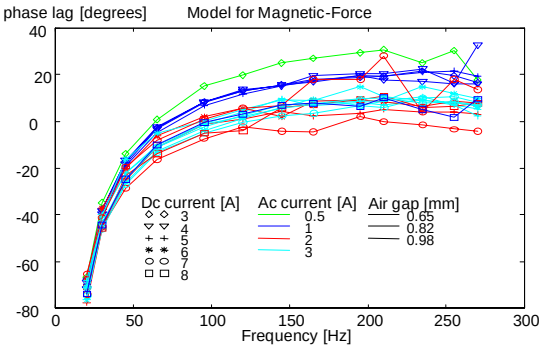

Figure 8. Phase lag of the magnetic force relative to equation 1 under different conditions: Current (AD/DC), and different air-gaps.

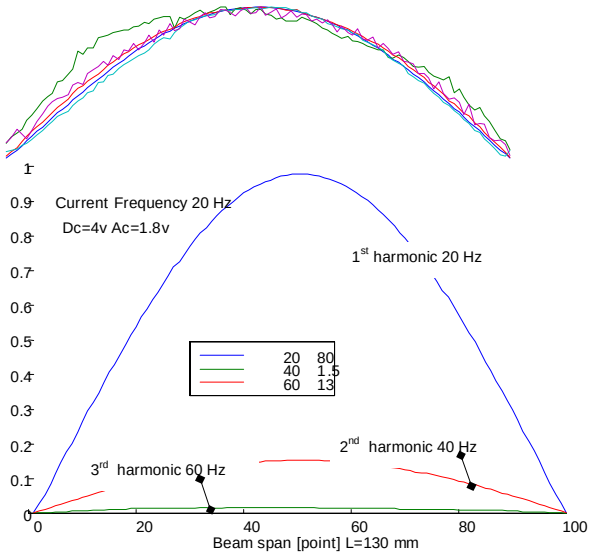

Figure 6. Bottom: Measured distribution of 3 normalized amplitude of the first 5 harmonics, showing a nearly identical amplitude distribution.

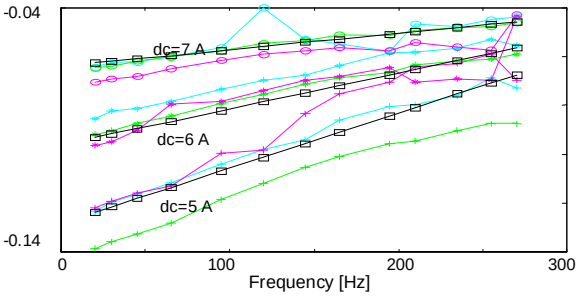

Figure 9. Agreement of estimated (generalized parameter) α wit equation 17.

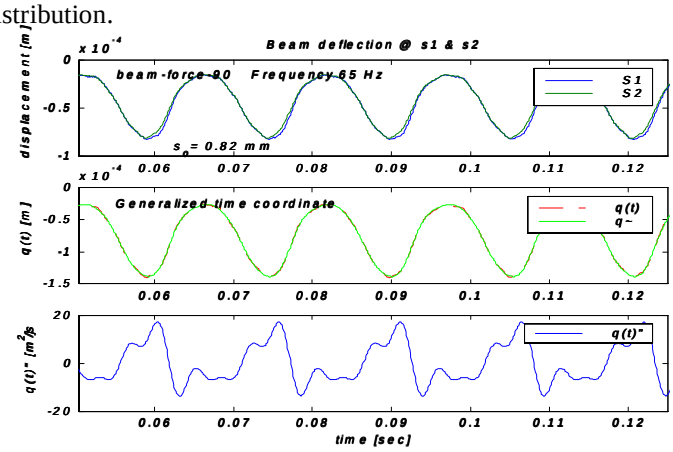

Figure 7. Top: measured and fitted displacements. Middle: reconstructed generalized cord. (eq. 15). Bottom: reconstructed generalized acceleration.